

Detecting protein analytes that modulate transmembrane movement of a polymer chain within a single protein pore

Liviu Movileanu^{1†}, Stefan Howorka^{1†}, Orit Braha¹, and Hagan Bayley^{1,2*}

¹Department of Medical Biochemistry and Genetics, The Texas A&M University System Health Science Center, College Station, TX 77843-1114.

²Department of Chemistry, Texas A&M University, College Station, TX 77843-3255. *Corresponding author (bayley@tamu.edu).

[†]These two authors contributed equally to this work.

Received 16 May 2000; accepted 26 June 2000

Here we describe a new type of biosensor element for detecting proteins in solution at nanomolar concentrations. We tethered a 3.4 kDa polyethylene glycol chain at a defined site within the lumen of the transmembrane protein pore formed by staphylococcal α -hemolysin. The free end of the polymer was covalently attached to a biotin molecule. On incorporation of the modified pore into a lipid bilayer, the biotinyl group moves from one side of the membrane to the other, and is detected by reversible capture with a mutant streptavidin. The capture events are observed as changes in ionic current passing through single pores in planar bilayers. Accordingly, the modified pore allows detection of a protein analyte at the single-molecule level, facilitating both quantification and identification through a distinctive current signature. The approach has higher time resolution compared with other kinetic measurements, such as those obtained by surface plasmon resonance.

Keywords: biosensor, nanostructure, polymer, pore, protein engineering

The continuing interest in nanotechnology has recently been extended to pioneering experimentation in designing functional nanostructures¹⁻³. Here we have engineered a protein-based structure in which a single functionalized polymer chain is attached at a defined site within the central cavity of a transmembrane pore self-assembled from staphylococcal α -hemolysin subunits. The untethered end of the polymer chain is capable of translocation across the membrane, from one entrance of the pore to the other, a distance of at least 10 nm. Hence, the engineered pore is an unusual nanostructure with a moveable part that can be used to examine the motions of single polymer chains on the microsecond time scale. We demonstrate here that the pore can act as a new type of biosensor element in which polymer-ligand conjugates are covalently attached to protein pores. A change in the ionic current carried by a modified pore occurs upon binding of a protein analyte to the functionalized polymer. The presentation of a ligand at the end of a polymer effectively solves the docking problem. Detection at the single-molecule level enables stochastic sensing, permitting both the quantification of an analyte, as well as its identification through a characteristic current signature.

α -Hemolysin (α HL), a toxin secreted by *Staphylococcus aureus* as a monomeric polypeptide of 293 amino acids, forms heptameric, mushroom-shaped pores of known three-dimensional structure in lipid bilayers^{4,5}. The opening of the channel on the cis side of the bilayer measures 29 Å in diameter and broadens into a cavity ~41 Å across (Fig. 1A). The cavity is connected to the transmembrane domain, a 14-stranded β -barrel with an average diameter of 20 Å. For applications in biotechnology, engineered versions of α HL have been prepared that contain built-in triggers and switches actuated by physical, chemical, and biochemical stimuli⁶⁻⁸. In addition, genetically engineered α HL and α HL in combination with noncovalent molecular adapters have been

used as stochastic sensor elements to monitor individual metal ions⁹ and small organic molecules¹⁰.

The interactions of polymers with various pores including α HL have been studied extensively¹¹⁻¹⁵. Recently, we devised an approach for the covalent attachment of single polyethylene glycol (PEG) molecules within the lumen of the α HL pore¹⁶. Now we have attached a functionalized polymer within the lumen. Measurements of the current passing through a single pore permit monitoring of the structural dynamics of the polymer chain. Because the polymer contains a biotinyl group at the untethered end, by using genetically engineered streptavidin mutants with a weakened binding affinity^{17,18}, we have been able to detect the appearance of the biotin on both the cis and trans sides of the membrane during a single experiment as distinctive capture events. Conversely, the frequency and nature of capture events can be used to identify and quantify proteins in solution.

Results and discussion

Preparation of an α HL pore containing a functionalized polymer.

Our preparation of heptameric α HL pores was enriched in molecules containing six unmodified subunits and *one* subunit covalently modified within the central cavity with PEG-biotin (Fig. 1B). Heptamers obtained by co-assembly^{9,16} of unmodified α HL and the mutant S106C, which had been reacted with biotin-PEG3400-maleimide (Fig. 1B, lane 2, band b), co-migrated with unmodified heptamers on sodium dodecyl sulfate-polyacrylamide gel electrophoresis (SDS-PAGE) (Fig. 1B, lane 1, band b). The addition of streptavidin (60 kDa) before electrophoresis caused ~75% of the material to migrate more slowly (Fig. 1B, lane 5, band c). This more slowly migrating material contained heteroheptamers with six unmodified and one modified subunit (H₆S106C-PEG-biotin), according to a second analysis by SDS-PAGE performed after heating the sample to dissociate the subunits (data not shown). No band

RESEARCH ARTICLES

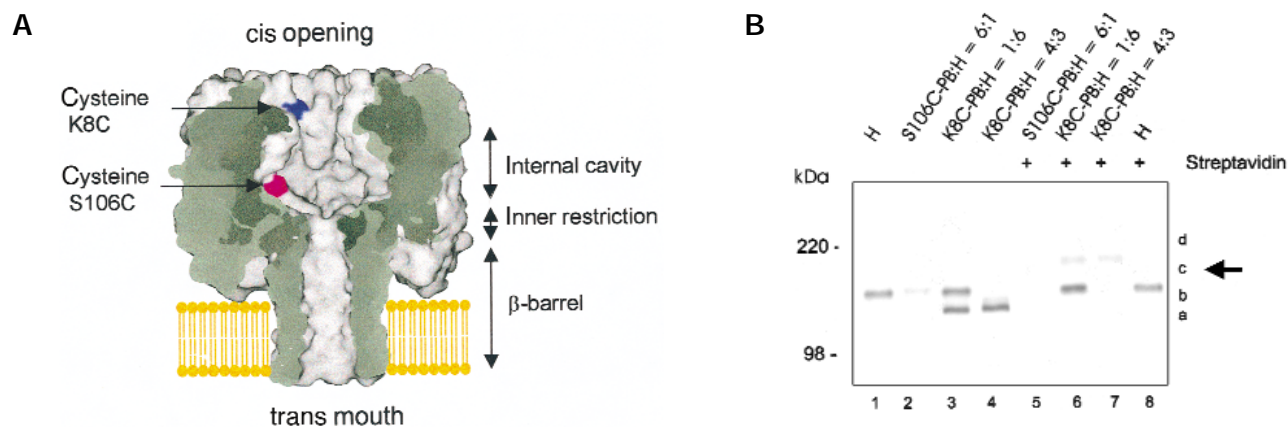


Figure 1. Preparation and analysis of heteroheptameric α HL pores. (A) Sagittal section of the α HL pore showing the positions of residues 8 and 106. (B) Analysis of heteroheptameric α HL pores. 35 S-labeled PEG-biotin-modified heteroheptamers were analyzed by SDS-PAGE and autoradiography. Where indicated, the samples were treated with excess WT-streptavidin before electrophoresis. The ratios of unmodified and modified subunits in the initial assembly mix are shown above each lane. The components of each band inferred from bandshifts after streptavidin treatment and dissociation of the subunits by heating followed by additional electrophoresis are as follows. Lane 1: band b, H₇; lane 2: band b, H₇ and mostly H₆106C-PEG-biotin₁; lane 3: band a, H₆K8C-PEG-biotin₁, band b, H₇; lane 4: band a, H₆K8C-PEG-biotin₁ (bands above band a contain H_{7-n}K8C-PEG-biotin_n with $n > 1$); lane 5: band b, H₇, band c, H₆106C-PEG-biotin₁ with streptavidin bound; lane 6: band b, H₇, band c, H₆K8C-PEG-biotin₁ with streptavidin bound; lane 7: band c, H₆K8C-PEG-biotin₁ with streptavidin bound (bands above c contain H_{7-n}K8C-PEG-biotin_n with $n > 1$ and streptavidin bound); lane 8: band b, H₇. By virtue of the bandshift produced by streptavidin, band c (arrow) represents the content of heteroheptamers with one PEG-biotin-modified subunit.

corresponding to heteroheptamers with two modified subunits was detected in the streptavidin-treated assembly products (Fig. 1B, lane 5), but such a band was present in a preparation of heteroheptamers derived from the mutant K8C modified with PEG-biotin (Fig. 1B, lane 7, band d). Position 8 is near the cis entrance to the channel lumen, and PEG molecules on all seven subunits can be tolerated at this position¹⁶.

Planar bilayer recordings with the modified pores. The single-channel properties of H₆106C-PEG-biotin₁ were examined by planar bilayer recording. Currents arising from the contaminating H₇ pores, which had the same conductance as control H₇ pores (271 ± 3 pS, $n = 14$), were disregarded (see Supplementary Material for a complete table of values obtained in the bilayer experiments: www.nature.com/nbt/current_issue/). The H₆106C-PEG-biotin₁ channels exhibited a reduced unitary conductance state (229 ± 4 pS, $n = 17$) decorated with short-lived high-amplitude negative spikes (mean lifetime, 130 ± 10 μ s, amplitude, 121 ± 4 pS, $n = 17$), which occurred at a high frequency (37 ± 6 s⁻¹, $n = 17$). Both the reduced conductance and the spikes were associated with the PEG chain (rather than the biotin), because H₆106C-PEG3K₁ channels, which contain a PEG of M_r 3,000 without the biotinyl group, showed very similar characteristics (unitary conductance 237 ± 4 pS; spike lifetime, 130 ± 10 μ s; amplitude, 128 ± 3 pS; frequency, 26 ± 10 s⁻¹, $n = 5$).

Capture of the tethered biotin by cis or trans streptavidin. When 12 nM wild-type (WT) streptavidin was added to the cis side of a bilayer containing a H₆106C-PEG-biotin₁ pore, the spikes disappeared completely after a lag period (120 ± 10 s, $n = 4$), leaving the mean conductance unchanged (Fig. 2A). By contrast, adding WT streptavidin to the trans side of the bilayer caused a permanent partial channel block of 120 ± 9 pS ($n = 5$) (Fig. 2B). The extent of the block ($51 \pm 3\%$, $n = 5$) was closely similar to the average amplitude of the short-lived spikes (121 ± 4 pS, $53 \pm 2\%$, $n = 17$) and occurred after a lag period of 160 ± 30 s ($n = 5$). The above results are interpreted as the essentially permanent capture of the PEG-biotin chain by WT streptavidin ($K_d = 4 \times 10^{-14}$ M in solution¹⁸) at the trans or cis side of the bilayer.

Reversible binding of the tethered biotin to a mutant streptavidin. Transient instead of permanent disappearances of the spikes were observed when W120A streptavidin, a mutant with consider-

ably lower affinity for biotin ($K_d = 1.1 \times 10^{-7}$ M, refs¹⁸⁻²⁰), was added to the trans or cis side of the H₆106C-PEG-biotin₁ pore (Fig. 2C, D). However, with regard to the extent of channel block, the transient binding events brought about by W120A were very similar to those seen with WT streptavidin: no measurable block on the cis side, and a $52 \pm 4\%$ block on the trans side. As expected for a bimolecular interaction, the frequency of occurrence of blocking events ($1/\tau_{on} = k_{on}[W120A]$) was proportional to the concentration of W120A (Fig. 2E, F).

Remarkably, the different signatures of the trans and cis events permitted us to monitor sequential binding events of W120A streptavidin from both sides of the bilayer in a single experiment (Fig. 2G, H). At identical protein concentrations, the reversible binding events of W120A streptavidin occurred far more frequently at the cis side than at the trans side. In addition, the trans events exhibited a shorter dwell time. Through the analysis of inter-event intervals (τ_{on}) and event lifetimes (τ_{off}), apparent kinetic constants (k) for the association and true kinetic constants (k) for the dissociation of the W120A streptavidin-biotin complex were obtained for each side of the lipid bilayer in 300 mM KCl, 5 mM Tris-HCl, pH 7.0, containing 100 μ M EDTA at +100 mV: $k'_{on,cis} = 3.8 \pm 0.3 \times 10^6$ M⁻¹ s⁻¹ (all k'_{on} values for streptavidin are corrected for the presence of four biotin binding sites on each protein); $k'_{off,cis} = 0.31 \pm 0.01$ s⁻¹; $K'_d,cis = 8.2 \pm 0.2 \times 10^{-8}$ M; $k'_{on,trans} = 1.1 \pm 0.2 \times 10^5$ M⁻¹ s⁻¹; $k'_{off,trans} = 1.5 \pm 0.6$ s⁻¹; $K'_d,trans = 1.4 \pm 0.6 \times 10^{-5}$ M. The value of K'_d,cis is closely similar to the reported K_d value (1.1×10^{-7} M)^{18,20}.

Interactions of the pore with a monoclonal antibody. Similar findings were obtained with a mouse anti-biotin monoclonal IgG₁ (mAb). For example, application of the mAb to the cis side of a bilayer containing H₆106C-PEG-biotin₁ was accompanied by the transient disappearance of the spikes but did not alter the amplitude of the main conductance state (data not shown). Because all three biotin-binding proteins fail to alter the unitary conductance when they bind on the cis side of the bilayer, it is likely that a major fraction of the PEG chain remains within the α HL cavity during cis captures. This conclusion is supported by electrophoretic analysis in which H₆106C-PEG-biotin₁ co-migrates with unmodified heptamers (H₇) (Fig. 1B, lanes 1 and 2, band b). By comparison, a single PEG5000 chain attached at position 106 increases the electrophoretic mobility of the heptamer and must protrude into the extraluminal solvent¹⁶.

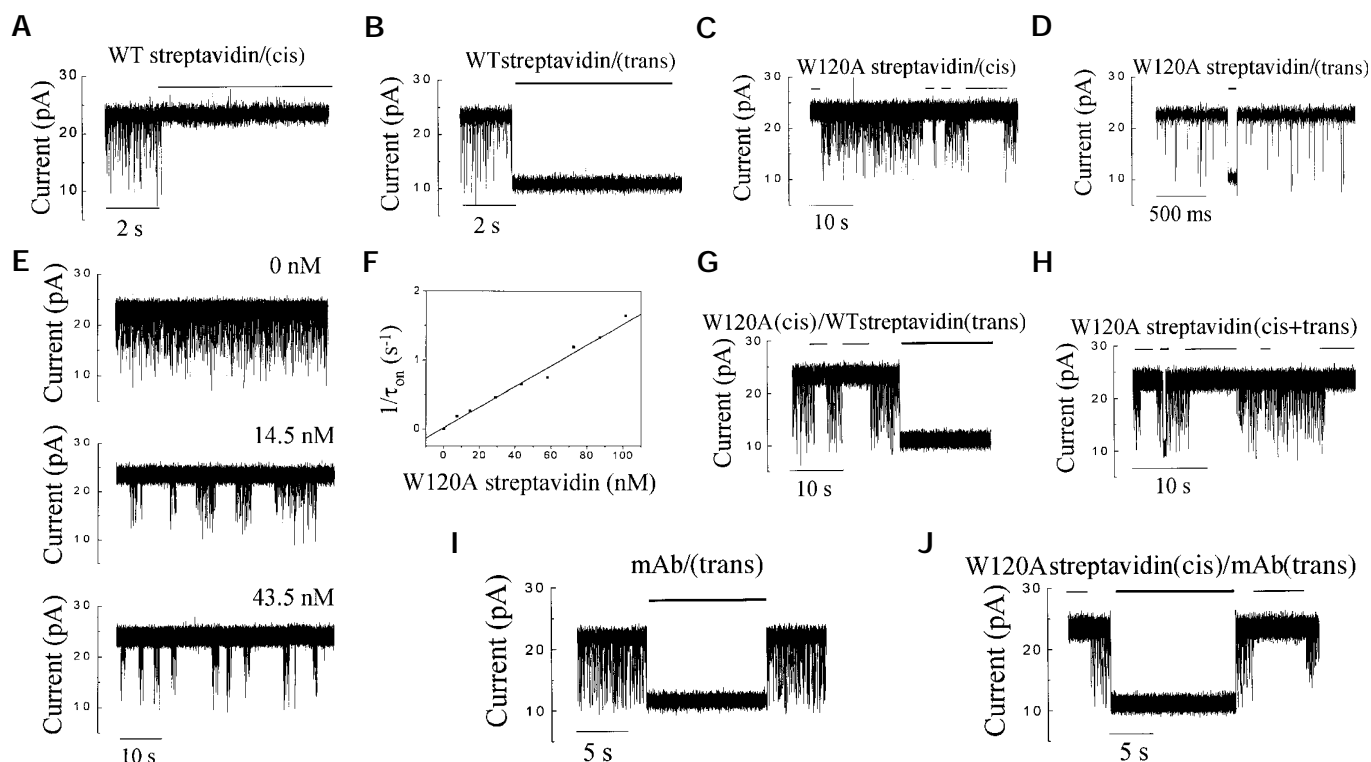


Figure 2. Response of $H_6106C\text{-PEG-biotin}_1$ to WT and W120A streptavidins and a mouse anti-biotin mAb. Single-channel current recordings. (A–D) Bars show biotin capture events. The streptavidins were added before the start of each trace. (A) WT streptavidin (12 nM) added to the cis chamber abolishes the high-amplitude spikes. (B) WT streptavidin (12 nM) added to the trans chamber leads to a permanent partial channel blockade closely similar in amplitude to the amplitude of the spikes. (C) W120A streptavidin (7.25 nM) added to the cis chamber leads to transient disappearances of the high-amplitude spikes, but does not alter the underlying current. (D) W120A streptavidin (7.25 nM) added to the trans chamber produces transient partial channel blockades closely similar in amplitude to the amplitude of the spikes. (E) The inter-event interval (τ_{on}) decreases with increasing cis W120A streptavidin. (F) Plot of $1/\tau_{on}$ versus cis W120A streptavidin concentration. Data from a typical experiment are plotted as a least-squares fit. In (G) and (H), the thick bars show trans biotin capture events and the thin bars cis events. The streptavidins were added before the start of each trace. (G) W120A streptavidin (7.25 nM) was added to the cis chamber and WT streptavidin (71.7 nM) to the trans chamber. Cis capture of biotin by W120A streptavidin produces transient disappearances of the spikes. By contrast, trans capture by WT streptavidin resulted in a permanent blockade. (H) W120A streptavidin (7.25 nM) was added to the cis chamber and W120A streptavidin (29 nM) was added to the trans chamber, producing transient events by capture on both the cis and trans sides. In (I) and (J), responses are shown to the mouse anti-biotin monoclonal IgG₁ (mAb no. 1297 597, Roche Molecular Biochemicals, Indianapolis, IN). Again, thick bars show trans biotin capture events and the thin bars cis events. The biotin-binding proteins were added before the start of each trace. (I) mAb (5.8 nM) was added to the trans chamber. A single capture event is shown. (J) mAb (29 nM) was added to the trans chamber with W120A streptavidin (7.25 nM) in the cis chamber. Both cis and trans capture events are seen.

Contrasting with cis capture, biotin capture by the mAb at the trans side of the bilayer led to a drop in the mean conductance of $55 \pm 2\%$ (Fig. 2I), close to the value for the streptavidins (W120A, $52 \pm 4\%$; WT, $51 \pm 3\%$). Because both the streptavidins and the mAb produce a similar block, it is likely that the physical origin of the block derives from the PEG chain passing through the inner restriction (Fig. 1), rather than from the binding protein itself. Kinetic constants for the association and dissociation of the mAb were obtained for both sides of the lipid bilayer in 300 mM KCl, 5 mM Tris-HCl, pH 7.00, containing 100 μ M EDTA at +100 mV: $k_{on}^{cis} = 4.9 \pm 1.0 \times 10^7 \text{ M}^{-1} \text{ s}^{-1}$ (all k_{on} values for the mAb are corrected for the presence of two biotin binding sites on each protein); $k_{off}^{cis} = 1.9 \pm 0.3 \times 10^{-2} \text{ s}^{-1}$; $K_d^{cis} = 3.9 \pm 0.6 \times 10^{-10} \text{ M}$; $k_{on}^{trans} = 4.3 \pm 1.0 \times 10^5 \text{ M}^{-1} \text{ s}^{-1}$; $k_{off}^{trans} = 2.9 \pm 0.7 \times 10^{-2} \text{ s}^{-1}$; $K_d^{trans} = 6.7 \pm 1.6 \times 10^{-8} \text{ M}$. Again, biotin-binding events could be observed on both sides of the bilayer in a single experiment. Indeed, captures by two different biotin-binding proteins were recorded, for example, cis: W120A streptavidin; trans: mAb (Fig. 2J). Finkelstein and colleagues have examined the transmembrane movement of biotinylated toxins by capture with streptavidin²¹, and we suggest that biotin-binding proteins with reduced affinity might have advantages in such studies, as demonstrated here.

A kinetic model for the interactions of the modified pore with proteins. The results with both W120A streptavidin and the monoclonal antibody are consistent with a simple kinetic model (Fig. 3 and Supplementary Material: www.nature.com/nbt/current_issue/). Because the biotinyl group is rarely captured on the trans side of the bilayer, we assume that k_{+}^{trans} is relatively small. Therefore, the fraction of time spent by the biotinyl group on the cis side is given by $p_{cis} = k_{+}^{cis} / (k_{+}^{cis} + k_{+}^{trans})$ and the fraction of time spent on the trans side by $p_{trans} = (k_{+}^{trans} / k_{+}^{trans}) \cdot (k_{-}^{cis} / (k_{-}^{cis} + k_{-}^{trans}))$. In terms of measurable dissociation constants $K_d^{cis} = p_{cis} K_d^{cis}$ and $K_d^{trans} = p_{trans} K_d^{trans}$. Therefore:

$$p_{cis} / p_{trans} = (K_d^{cis} / K_d^{trans}) \cdot (K_d^{trans} / K_d^{cis}) \quad (1)$$

Assuming that the dissociation constants for the biotin/streptavidin interaction are the same as those determined under other circumstances¹⁸ and the same on both sides of the bilayer ($K_d^{cis} = K_d^{trans}$), we find that $p_{cis} / p_{trans} = 170 \pm 70$. The latter assumption is not strictly true; for example, for streptavidin W120A, k_{off}^{trans} is about five times larger than k_{off}^{cis} . Perhaps elongation of the PEG chain lowers the activation barrier for dissociation. Whereas the value of p_{cis} / p_{trans} is approximate, it does provide a qualitative picture of biotin localization with respect to the bilayer. It is reassuring

RESEARCH ARTICLES

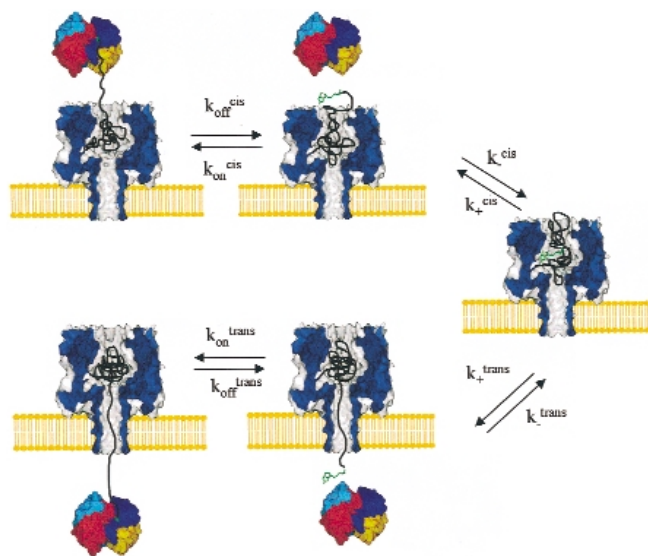


Figure 3. Kinetic model of the interactions between the α HL pore H₆106C-PEG-biotin₁ and streptavidin at the cis and trans sides of the bilayer. The α HL pore and tetrameric streptavidin are shown to scale.

to find that equation 1 yields a similar value of $p_{\text{cis}}/p_{\text{trans}} = 170 \pm 40$ for experiments with the mAb.

When the biotinyl group is captured on the cis side of the bilayer by the streptavidins or the mAb, there is no detectable change in channel conductance, suggesting that the PEG chain is still largely contained within the central cavity, where it reduces the flow of ions by about 15.5%¹⁶, and that the streptavidin molecule does not itself perturb current flow. By contrast, capture on the trans side is accompanied by a dramatic reduction in single-channel conductance that is strikingly similar in amplitude to the current reduction seen during the transient current spikes that occur in the absence of the biotin-binding proteins or between captures in their presence. This similarity indicates that the spikes represent excursions of the biotinyl group toward the trans entrance into the transmembrane β -barrel. In accordance with this interpretation, there is a complete absence of spikes during the cis capture events when the end of the polymer is unavailable for threading into the barrel. The spikes occupy about 0.48% of the current trace in the absence of streptavidin, which is roughly in accord with the value of $p_{\text{cis}}/p_{\text{trans}}$. Therefore, the frequency of occurrence of the spikes of $37 \pm 6 \text{ s}^{-1}$ is likely to be the upper limit for the rate of appearance at the trans entrance and for transmembrane movement (appearances at the cis entrance being more frequent but electrically silent). The time required for a PEG chain of M_r 2,000 to sample a near fully extended conformation has been calculated to be in the range of a few milliseconds²².

The modified pore as a sensor element for detecting protein analytes. Importantly, our results show how engineered protein pores can be used, at the single-molecule level, as stochastic sensor elements²³ for protein analytes. We had previously used modified α HL pores to detect divalent metal ions⁹ and organic molecules¹⁰. Here we have shown that proteins such as antibodies (Fig. 2I) can be detected using a chemically modified pore. Proteins are quantified at low nanomolar concentrations by the linear relationship between $1/\tau_{\text{on}}$ and concentration (Fig. 2F). The use of biotin is illustrative of the wide variety of immobilized ligands that might be used. The technology we have described has advantages over other sensing devices that measure kinetic parameters, such as surface plasmon resonance. For example, stochastic sensing with single pores can readily yield dwell times as short

as 100 μs and does not present the difficulties associated with crowded or heterogeneous surfaces on sensor chips²⁴.

Prospects. We have assembled a nanoscale protein pore with a covalently attached and functionalized moving arm (Fig. 3). The untethered end of the arm, which is $\sim 27 \text{ nm}$ in length when outstretched, is free to move across the bilayer from one mouth of the pore to the other, a distance of $>10 \text{ nm}$. Despite the great interest in nanostructures, few assemblies with moving parts have been made; one recent achievement is a nanomechanical device based on the B-Z transition of DNA²⁵. Future developments of our functionalized pore might include the ability to control the position of an arm, for example with the applied transmembrane voltage, and thereby drive transmembrane transport. The system we have developed also has potential for the examination of the dynamics of polymers other than PEG at the single-molecule level, including biological molecules such as polynucleotides, oligosaccharides, and peptides. The characterization of single-polymer molecules is an active area of research that is usually limited to optical microscopy or force measurements^{26–29}. Finally, we have shown that pores with tethered functionalized polymers can be used as components for stochastic sensing. Stimulus-responsive polymers³⁰ might also be attached in the channel lumen to yield another class of sensor elements.

Experimental protocol

Formation of heteromeric α HL pores containing covalently attached PEG-biotin. The mutant α HL genes, S106C, K8C, and K8A, have been described (ref. 31–33). ³⁵S-labeled S106C, K8C, and K8A polypeptides were obtained by in vitro transcription and translation³⁴. To obtain a higher yield of protein, unlabeled methionine was included in the expression mix^{33,34}. α HL monomers S106C and K8C were covalently modified by fivefold dilution of the translation mix into 10 mM MOPS (3-[N-morpholino]propanesulfonic acid), pH 7.0 (NaOH), containing 150 mM NaCl, 0.5 mM EDTA, reduction with 0.5 mM dithiothreitol (DTT) for 5 min, and reaction with 10 mM biotin-PEG3400-maleimide (Shearwater Polymers, Huntsville, AL) for 10 min at room temperature. Modified subunits were mixed in various ratios with unmodified K8A α HL monomers (H) and allowed to assemble into heteroheptamers on rabbit erythrocyte membranes^{33,34}. α HL heptamers are stable in SDS unless heated³⁵, and were analyzed by SDS-PAGE and autoradiography. Where indicated a large excess (8.5 mg/ml) of streptavidin (S-4762; Sigma Chemical Co., St. Louis, MO) was added before analysis. Heptameric pores for electrical recording were obtained from preparative gels⁹. The ratios of unmodified to modified subunits in these purified proteins were determined by heating the proteins to 95°C and separating the dissociated subunits in a second, analytical gel¹⁶.

Bilayer recording. The formation of bilayers of 1,2-diphytanoyl-*sn*-glycerophosphocholine (Avanti Polar Lipids, Alabaster, AL), the insertion of heptameric α HL pores into them, and single-channel recording have been described^{9,36}. Both the cis and trans chambers of the apparatus contained 300 mM KCl, 5 mM Tris-HCl, pH 7.0, with 100 μM EDTA. α HL pores were added to the cis chamber, at a concentration of 0.05–0.3 ng/ml. The solution was stirred for $\sim 15 \text{ min}$ until a single channel inserted into the bilayer. Currents were recorded by using a patch clamp amplifier (Axopatch 200B, Axon Instruments, Foster City, CA) at a holding potential of +100 mV (with the cis side grounded). The signals were low-pass filtered with a built-in four-pole Bessel filter at a frequency of 10 kHz and recorded on digital audio tape recorder. For computer analysis, the signals were further filtered with an eight-pole low-pass Bessel filter (Frequency Devices, Haverhill, MA) at frequencies in the range 1–4 kHz and sampled at 20 kHz. Statistical analysis was carried out by using the FETCHAN and pSTAT programs, both from the software package pCLAMP7 (Axon Instruments), and Origin (Microcal Software, Northampton, MA). Measurements are given as mean \pm s.d. $k_{\text{off}}^{\text{cis}}$ values were obtained from $1/\tau_{\text{off}}$, determined from dwell-time histograms. $k_{\text{on}}^{\text{cis}}$ values were determined from the concentration dependence of $1/\tau_{\text{on}}$. Because relatively few events were recorded, $k_{\text{off}}^{\text{trans}}$ and $k_{\text{on}}^{\text{trans}}$ values were determined from mean dwell times and mean inter-event intervals. For cis events, n refers to the number of experiments. For trans events, n refers to the number of events.

Molecular graphics. The molecular models of streptavidin (1swd.pdb) and α -hemolysin (7ahl.pdb) were generated with SPOCK 6.3 software³⁷.

Acknowledgments

We are most grateful to Pat Stayton and David Hyre for the W120A protein. This work was supported by a Multidisciplinary University Research Initiative (MURI) award (Office of Naval Research) to H.B., a MURI award (Air Force Office of Scientific Research) to A.J. Welch, the Department of Energy and the Texas Advanced Technology Program. S.H. holds a postdoctoral fellowship from the Austrian Science Foundation (Fonds zur Förderung der wissenschaftlichen Forschung). We thank Li-Qun Gu, Yong Zhang, and Sean Conlan for their help and suggestions.

1. Heath, J.R., Kuekes, P.J., Snider, G.S. & Williams, R.S. A defect-tolerant computer architecture: opportunities for nanotechnology. *Science* **280**, 1716–1721 (1998).
2. Davis, A.P. Synthetic molecular motors. *Nature* **401**, 120–121 (1999).
3. Seeman, N.C. DNA engineering and its applications to nanotechnology. *Trends Biotechnol.* **17**, 437–443 (1999).
4. Song, L. *et al.* Structure of staphylococcal α -hemolysin, a heptameric transmembrane pore. *Science* **274**, 1859–1865 (1996).
5. Gouaux, E. α -Hemolysin from *Staphylococcus aureus*: an archetype of β -barrel, channel-forming toxins. *J. Struct. Biol.* **121**, 110–122 (1998).
6. Chang, C.-Y., Niblack, B., Walker, B. & Bayley, H. A photogenerated pore-forming protein. *Chem. Biol.* **2**, 391–400 (1995).
7. Panchal, R.G., Cusack, E., Cheley, S. & Bayley, H. Tumor protease-activated, pore-forming toxins from a combinatorial library. *Nat. Biotechnol.* **14**, 852–856 (1996).
8. Russo, M.J., Bayley, H. & Toner, M. Reversible permeabilization of plasma membranes with an engineered switchable pore. *Nat. Biotechnol.* **15**, 278–282 (1997).
9. Braha, O. *et al.* Designed protein pores as components for biosensors. *Chem. Biol.* **4**, 497–505 (1997).
10. Gu, L.-Q., Braha, O., Conlan, S., Cheley, S. & Bayley, H. Stochastic sensing of organic analytes by a pore-forming protein containing a molecular adapter. *Nature* **398**, 686–690 (1999).
11. Bezrukov, S.M., Vodyanoy, I. & Parsegian, V.A. Counting polymers moving through a single ion channel. *Nature* **370**, 279–281 (1994).
12. Bezrukov, S.M., Vodyanoy, I., Brutyan, R.A. & Kasianowicz, J.J. Dynamics and free energy of polymer partitioning into a nanoscale pore. *Macromolecules* **29**, 8517–8522 (1996).
13. Merzlyak, P.G. *et al.* Polymeric nonelectrolytes to probe pore geometry: application to the α -toxin transmembrane channel. *Biophys. J.* **77**, 3023–3033 (1999).
14. Kasianowicz, J.J., Brandin, E., Branton, D. & Deamer, D.W. Characterization of individual polynucleotide molecules using a membrane channel. *Proc. Natl. Acad. Sci. USA* **93**, 13770–13773 (1996).
15. Akeson, M., Branton, D., Kasianowicz, J.J., Brandin, E. & Deamer, D.W. Microsecond time-scale discrimination among polycytidylic acid, polyadenylic acid and polyuridylic acid as homopolymers or as segments within single RNA molecules. *Biophys. J.* **77**, 3227–3233 (1999).
16. Howorka, S. *et al.* A protein pore with a single polymer chain tethered within the lumen. *J. Am. Chem. Soc.* **122**, 2411–2416 (2000).
17. Sano, T. & Cantor, C.R. Intersubunit contacts made by tryptophan 120 with biotin are essential for both strong biotin binding and biotin-induced tighter subunit association of streptavidin. *Proc. Natl. Acad. Sci. USA* **92**, 3180–3184 (1995).
18. Chilkoti, A., Tan, P.H. & Stayton, P.S. Site-directed mutagenesis studies of the high-affinity streptavidin–biotin complex: contributions of tryptophan residues 79, 108, and 120. *Proc. Natl. Acad. Sci. USA* **92**, 1754–1758 (1995).
19. Chilkoti, A., Boland, T., Ratner, B.D. & Stayton, P.S. The relationship between ligand-binding thermodynamics and protein–ligand interaction forces measured by atomic force microscopy. *Biophys. J.* **69**, 2125–2130 (1995).
20. Pérez-Luna, V.H. *et al.* Molecular recognition between genetically engineered streptavidin and surface-bound biotin. *J. Am. Chem. Soc.* **121**, 6469–6478 (1999).
21. Slatin, S.L., Qiu, X.-Q., Jakes, K.S. & Finkelstein, A. Identification of a translocated protein segment in a voltage-dependent channel. *Nature* **371**, 158–161 (1994).
22. Wong, J.Y., Kuhl, T.L., Israelachvili, J.N., Mullah, N. & Zalipsky, S. Direct measurement of a tethered ligand–receptor interaction potential. *Science* **275**, 820–822 (1997).
23. Bayley, H., Braha, O. & Gu, L.-Q. Stochastic sensing with protein pores. *Adv. Mater.* **12**, 139–142 (2000).
24. Myszkka, D.G. Improving biosensor design. *J. Mol. Recognition* **12**, 279–284 (1999).
25. Mao, C., Sun, W., Shen, Z. & Seeman, N.C. A nanomechanical device based on the B–Z transition of DNA. *Nature* **397**, 144–146 (1999).
26. Weiss, S. Fluorescence spectroscopy of single biomolecules. *Science* **283**, 1676–1683 (1999).
27. Mehta, A.D., Rief, M., Spudich, J.A., Smith, D.A. & Simmons, R.M. Single-molecule biomechanics with optical methods. *Science* **283**, 1689–1695 (1999).
28. Xie, X.S. & Lu, H.P. Single-molecule enzymology. *J. Biol. Chem.* **274**, 15967–15970 (1999).
29. Marszalek, P.E. *et al.* Mechanical unfolding intermediates in titin molecules. *Nature* **402**, 100–103 (1999).
30. Stayton, P.S. *et al.* Control of protein–ligand recognition using a stimuli-responsive polymer. *Nature* **378**, 472–474 (1995).
31. Walker, B.J. & Bayley, H. A pore-forming protein with a protease-activated trigger. *Protein Eng.* **7**, 91–97 (1994).
32. Walker, B. & Bayley, H. Key residues for membrane binding, oligomerization, and pore-forming activity of staphylococcal α -hemolysin identified by cysteine scanning mutagenesis and targeted chemical modification. *J. Biol. Chem.* **270**, 23065–23071 (1995).
33. Cheley, S., Braha, O., Lu, X., Conlan, S., & Bayley, H. A functional protein pore with a “retro” transmembrane domain. *Protein Sci.* **8**, 1257–1267 (1999).
34. Walker, B.J., Krishnaswamy, M., Zorn, L., Kasianowicz, J.J. & Bayley, H. Functional expression of the α -hemolysin of *Staphylococcus aureus* in intact *Escherichia coli* and in cell lysates. *J. Biol. Chem.* **267**, 10902–10909 (1992).
35. Walker, B. & Bayley, H. Restoration of pore-forming activity in staphylococcal α -hemolysin by targeted chemical modification. *Protein Eng.* **8**, 491–495 (1995).
36. Montal, M. & Mueller, P. Formation of bimolecular membranes from lipid monolayers and study of their electrical properties. *Proc. Natl. Acad. Sci. USA* **69**, 3561–3566 (1972).
37. Christopher, J.A. *SPOCK: the structural properties observation and calculation kit* (program manual). (Center for Macromolecular Design, Texas A&M University, College Station, TX; 1998).